THE JOURNAL OF PHYSICAL CHEMISTRY A

Article

pubs.acs.org/JPCA

J. Phys. Chem. A 117, 9704 (2013)

Potential Curves for the Dissociative Recombination of CO^+

Steven L. Guberman*

Institute for Scientific Research, 22 Bonad Road, Winchester, Massachusetts 01890, United States

ABSTRACT: Large scale ab initio calculations are reported for the diabatic $^3\Pi$, $^1\Pi$, $^1\Sigma^+$, $^1\Delta$, $^3\Sigma^+$, and $^3\Delta$ valence states of CO that provide routes for the dissociative recombination of the ground electronic and vibrational state of CO^+. The most important routes are $2^3\Pi$, $3^3\Pi$, $2^1\Pi$, and $D'^1\Sigma^+$. For electron energies below 0.2961 eV, from the $v = 0$ ion level, the first two states can generate excited atoms, $O(^1D)$ and $C(^1D)$, but the last two states yield only ground state atoms. From $v = 0$, hot ground state atoms are generated at 0 eV from each of the four states with C and O having 1.67 and 1.25 eV of kinetic energy, respectively. The potential curves are compared to prior calculations and experiments.

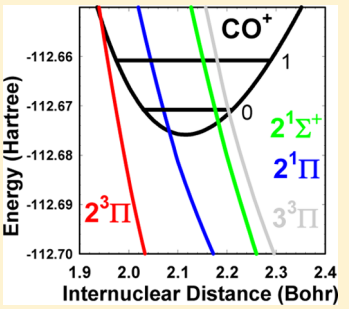

I. INTRODUCTION

CO^+ has been detected in planetary nebulae,[1] and dissociative recombination (DR)

$$CO^+ + e^- \rightarrow C + O \quad (1)$$

may be the dominant destruction mechanism. CO^+ is a major species in the plasma tail of comets, and DR has been included in detailed models of comet atmospheres.[2] DR was proposed as a source of C in the inner coma and as a source of C ($^1D \rightarrow {}^3P$) emission at 1931 Å in comet spectra.[3] The interpretation of comet Halley measurements has included CO^+ DR[4] as has another model of a diamagnetic cavity surrounding the nucleus.[5] The Pioneer Venus Orbiter Ultraviolet Spectrometer observed a hot C corona due in part to DR.[6] At Mars, DR of CO^+ isotopomers is a source of atomic isotope enrichment.[7] DR of CO^+ is the main source of C and O in the Triton ionosphere.[8]

The ab initio calculation of DR cross sections and rate constants requires potential curves for the ion on the left side of eq 1 and for the dissociative routes on the right side. The calculation of these potential curves is the subject of this paper. Under most conditions, including those in planetary ionospheres, planetary nebulae, interstellar clouds, and laboratory experiments, CO^+ will radiatively relax to the $v = 0$ level of the ground state before it can recombine with an electron. Therefore, DR of only the $v = 0$ ion level is considered here.

In section II, the calculation of the potential curves is described. The atomic products of DR are discussed in section III. There have been many prior determinations of potential curves and spectroscopic constants from other theory and experiments, and these are compared to the present work in section IV. The conclusions are in section V.

II. POTENTIAL CURVES

A. CO^+ and CO Ground States. The potential curves have been calculated with a cc-pVQZ Gaussian basis set[9] on the C and the O using the MOLPRO programs.[10] The main configuration near R_e in the $X^2\Sigma^+$ state of CO^+ is $1\sigma^2 2\sigma^2 3\sigma^2 4\sigma^2 5\sigma 1\pi_+^2 1\pi_-^2$. The orbitals were determined in complete active space self-consistent field (CASSCF)[11] calculations in which 1σ and 2σ were kept fully occupied and the active space consisted of the 3σ–6σ, 1π, and 2π orbitals. The ion orbitals were optimized for the $X^2\Sigma^+$ state. The internally contracted multireference configuration interaction (MRCI)[12] wave function was calculated by generating all single and double excitations from the full CASSCF wave function, keeping the 1σ and 2σ orbitals fully occupied in all configurations. A single root was determined in the MRCI for $R \leq 4.6a_0$. The lowest root is $^2\Delta$ for $R > 4.6a_0$. In a two-root MRCI, the lowest root at $R > 4.6a_0$ is $X^2\Sigma^+$ and the second root is $^2\Delta$. Therefore, a two-root MRCI was done for $R > 4.6a_0$. Because of the nature of the MRCI approach, this leads to a slight inconsistency with the energies at smaller R, but the difference is very small. The ion energies are given in Table 1, and the calculated properties are compared to experiment[13] in Table 2. All reported energies are from the MRCI including the Davidson correction. Table 2 also has properties for the CO ground state calculated by an equivalent approach with orbitals optimized for the ground state. The calculated neutral ground state energy at R_e is −113.189 044 au. The ionization energy relative to the calculated ground state and the ion fundamental frequency are only 0.05 eV and 14 cm^{-1} too low, respectively, and the equilibrium internuclear separation is only $0.0083a_0$ greater than experiment. For the neutral ground state, the differences from experiment are similar to those for the ion except for the anharmonicity, which is described better in the ground state.

B. Neutral Excited States. The mechanism for dissociative recombination in CO^+ requires that the dissociative curves

Special Issue: Oka Festschrift: Celebrating 45 Years of Astrochemistry

Received: December 15, 2012
Revised: March 20, 2013

   dx.doi.org/10.1021/jp312359c | J. Phys. Chem. A XXXX, XXX, XXX–XXX

Table 1. Energies[a] for CO^+, $X^2\Sigma^+$

R (bohr)	energy (au)	R (bohr)	energy (au)
1.550	−0.225 473	2.6	−0.595 369
1.575	−0.279 967	2.65	−0.583 471
1.600	−0.329 251	2.7	−0.571 593
1.625	−0.373 736	2.75	−0.559 829
1.65	−0.413 802	2.8	−0.548 255
1.675	−0.449 800	2.85	−0.536 937
1.70	−0.482 053	2.9	−0.525 927
1.725	−0.510 860	2.95	−0.515 268
1.75	−0.536 497	3.1	−0.485 708
1.775	−0.559 218	3.2	−0.468 230
1.80	−0.579 259	3.3	−0.452 651
1.825	−0.596 838 1	3.4	−0.439 009
1.85	−0.612 156	3.5	−0.427 286
1.875	−0.625 397	3.6	−0.417 392
1.9	−0.636 736	3.7	−0.409 103
1.925	−0.646 330	3.8	−0.402 152
1.95	−0.654 327	3.9	−0.396 355
1.975	−0.660 862	4	−0.391 560
2	−0.666 061	4.2	−0.384 400
2.025	−0.670 042	4.4	−0.379 581
2.05	−0.672 910	4.6	−0.376 291
2.075	−0.674 766	4.8	−0.374 328
2.1	−0.675 701	5	−0.372 686
2.125	−0.675 802	5.2	−0.371 507
2.15	−0.675 146	5.4	−0.370 653
2.175	−0.673 806	5.6	−0.370 030
2.2	−0.671 850	5.8	−0.369 573
2.225	−0.669 339	6.0	−0.369 238
2.25	−0.666 331	6.2	−0.368 990
2.275	−0.662 879	6.4	−0.368 805
2.3	−0.659 031	6.6	−0.368 668
2.325	−0.654 834	6.8	−0.368 565 4
2.35	−0.650 328	7.0	−0.368 489
2.375	−0.645 551	7.2	−0.368 433
2.4	−0.640 539	7.4	−0.368 392
2.425	−0.635 325	7.6	−0.368 362
2.45	−0.629 938	7.8	−0.368 340
2.55	−0.607 174	8.0	−0.368 328

[a]Add −112 to get the total energy.

cross the ion potential energy curve. This requires the use of diabatic states, i.e., neutral states from which the ion ground state has been projected out. Without this projection, the neutral states would have avoided crossings with Rydberg states and would not cross the ion. This projection is accomplished approximately by omitting diffuse character in the basis set. This effectively removes, for energies near the ion, all character that is primarily the ground or excited ion state plus a diffuse Rydberg orbital. The degree of Rydberg−valence mixing varies with the electronic symmetry, and this is discussed below. Because Rydberg character is intentionally omitted, the calculated spectroscopic constants may not agree favorably with experiment for states that have considerable Rydberg−valence mixing. For the neutral states, the orbitals and the CI wave functions were determined using the same approach as described for the ion. For each electronic symmetry, the CASSCF orbitals were optimized for that symmetry.

The importance of a dissociative state is in part determined by whether the repulsive wall comes close enough to the $v = 0$ ion turning points to make a significant contribution to the cross section through either the direct or the indirect DR mechanisms. Recently, for N_2^+ DR,[14] I found that a useful criterion for selecting dissociative states involves an examination of a high vibrational level of the lowest Rydberg state of the same electronic symmetry. If the level falls above $v = 0$, and the dissociative curve crosses the Rydberg state near the turning points of that level, then that state may provide a route for DR by the indirect mechanism. This criterion does not require that the repulsive curve cross the ion but does require another repulsive curve of the same electronic symmetry to have a favorable ion crossing. Initial capture occurs into the favorable ion crossing state followed by transfer to the unfavorable state via the intermediate Rydberg state. For N_2^+, I found that the $C^3\Pi_u$ state, at the energy of the $v = 0$ ion level, is near the inner turning point of the $v = 11$ level of the $n = 3$ $G^3\Pi_u$ state and $0.2a_0$ to smaller R from the inner turning point of $v = 0$. Nevertheless, this dissociative route contributed 13% of the total cross section near the energy of $v = 11$.

There are four atomic asymptotes that can provide routes for DR from the $v = 0$ ion level near zero electron energy. Because of the $^2\Sigma^+$ symmetry of the ion ground state, only singlet and triplet states are likely dissociative routes. States of Σ^-, Φ, and

Table 2. Spectroscopic Results for CO and CO^+ Diabatic States Compared to Experiment[13]

state	T_e (eV)	ω_e (cm^{-1})	$\omega_e x_e$ (cm^{-1})	R_e (bohr)
CO^+, $X^2\Sigma^+$	13.96 (14.01)	2200 (2214)	18.25 (15.16)	2.1156 (2.1073)
CO, $2^1\Delta$	14.30	963	37.1	2.6677
CO, $3^1\Sigma^+$	13.26	654	6.83	3.5577
CO, $3^1\Pi$	13.03	492	−30.19	3.5965
CO, $2^1\Pi$	12.43	1116	16.99	2.5347
CO, $3^3\Pi$	12.40	1259	59.97	2.6041
CO, $3^3\Pi$[c]	12.08	422.4	69.74	3.8828
CO, $2^3\Pi$	11.26 (11.28)[b]	816.3 (805.1)[b]	4.67 (−2.85)[b]	2.6248
CO, $D'^1\Sigma^+$	11.11 (11.09)[a]	523.9 (651.4)[a]	52.64 (20.4)[a]	3.0895 (2.991)[a]
CO, $A^1\Pi$	8.09 (8.07)	1521 (1518)	27.69 (19.40)	2.3426 (2.3344)
CO, $D^1\Delta$	8.06 (8.10)	1080 (1094.0)	9.26 (10.20)	2.6603 (2.6437)
CO, $d^3\Delta$	7.43 (7.58)	1181 (1171)	9.67 (10.63)	2.6113 (2.5882)
CO, $a'^3\Sigma^+$	6.76 (6.92)	1229 (1228)	9.82 (10.468)	2.5837 (2.5555)
CO, $a^3\Pi$	6.07 (6.03)	1733 (1743)	13.76 (14.36)	2.2881 (2.2785)
CO, $X^1\Sigma^+$		2151 (2169)	12.54 (13.29)	2.1394 (2.1322)

[a]From ref 32. [b]From ref 16. [c]This is the outer adiabatic well.

dx.doi.org/10.1021/jp312359c | J. Phys. Chem. A XXXX, XXX, XXX−XXX

Γ symmetry will have only very small electronic capture widths and can be neglected. With these considerations, from the ground states of the separated atoms there are $X^1\Sigma^+$, $D'^1\Sigma^+$, $a'^3\Sigma^+$, $2^3\Sigma^+$, $A^1\Pi$, $2^1\Pi$, $a^3\Pi$, $2^3\Pi$, and the bound $D^1\Delta$ and $d^3\Delta$ states. Both the second asymptote, $C(^1D) + O(^3P)$, and the third energetically possible asymptote, $C(^3P) + O(^1D)$, yield one $^3\Sigma^+$, two $^3\Delta$, and three $^3\Pi$ states. The fourth asymptote, $C(^1S) + O(^3P)$, yields a $^3\Pi$ state. The next asymptote, $C(^1D) + O(^1D)$, lies at 0.2961 eV[13,15] above $v = 0$ and gives rise to $3^1\Delta$, $4^1\Pi$, and $3^1\Sigma^+$ states. Several of the above states are well-known and bound and will not be important routes for DR.

The calculated $^3\Pi$ potential curves are shown in Figure 1. The CASSCF active space is the same as that for the ion. The CASSCF calculations are done in an average of $^3B_1$ and $^3B_2$ symmetry of C_{2v} so that the π_x and π_y orbitals are equivalent. The orbitals are obtained from an eight-root average in the CASSCF. Eight roots are obtained in the MRCI in $^3B_1$ symmetry. The MRCI energies including the Davidson correction are given in Table 3 for $2^3\Pi$ and $3^3\Pi$. The $^3\Phi$ curve is also a product of the calculations and is shown in Figure 1, although it plays no role in DR. The $a^3\Pi$ potential curve is partially shown in Figure 1 and is too low in energy for DR. Its spectroscopic constants (see Table 2) are comparable in accuracy to those for the ion except for $\omega_e x_e$ and provide confidence that the other $^3\Pi$ curves are as accurate. Note that $a^3\Pi$ has a hump of 245 cm^{-1} at $4.5954a_0$. $2^3\Pi$ has an avoided crossing with $3^3\Pi$ near $3.5a_0$. Both states have wells with minima at $2.6248a_0$ and $2.6041a_0$, respectively (see Table 2). These purely valence potential curves have minima that lie above their asymptotes (see Figure 1), indicating that the vibrational levels may be short-lived. Based upon the widths of the barriers, the low levels of $2^3\Pi$ should have longer lifetimes than those of $3^3\Pi$. The T_e and ω_e values for $2^3\Pi$ are in excellent agreement with experiment.[16] Also reported in Table 2 are spectroscopic constants for the $3^3\Pi$ outer well.

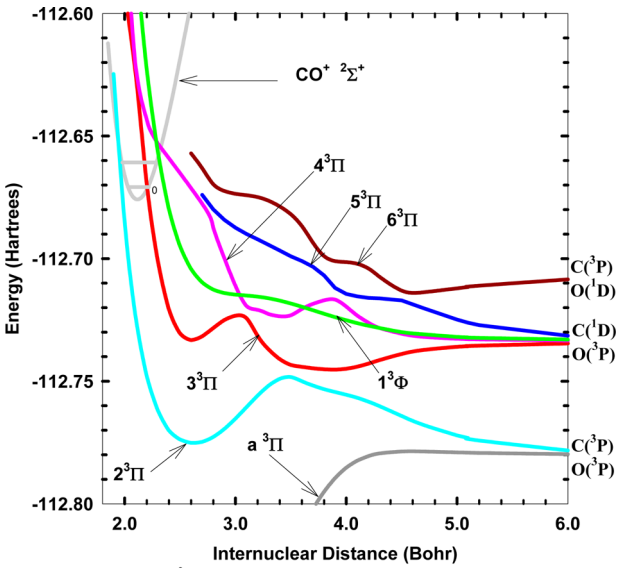

Figure 1. $^3\Pi$ and $^3\Phi$ states of CO with the ion ground state.

From the $v = 0$ ion level at low electron energies, it is clear from Figure 1 that only the $2^3\Pi$ and $3^3\Pi$ states will play a role. $4^3\Pi$ is too far to large R, at the $v = 0$ energy, to play a role at low energy, but it could contribute at electron energies near 0.5 eV.

The $^1\Pi$ curves were calculated with the same approach as for $^3\Pi$ except that six roots for both $^1B_1$ and $^1B_2$ were averaged for determination of the orbitals and six roots were obtained in the MRCI. The MRCI energies with the Davidson correction for $2^1\Pi$ are in Table 3. A portion of the $A^1\Pi$ curve is shown in Figure 2. Although it is too low in energy to contribute to DR, its calculated spectroscopic constants (see Table 2), especially T_e and ω_e, are excellent. The A state has a hump of 543 cm^{-1} found here at $4.3081a_0$. $2^1\Pi$ has an avoided crossing with $3^1\Pi$ near $3.3a_0$. The peak of the hump in $2^1\Pi$ is at $3.2a_0$ and is 1.94

Table 3. Energies (au)[a] for $2^3\Pi$ and $3^3\Pi$

R (bohr)	$2^3\Pi$	$3^3\Pi$	R (bohr)	$2^3\Pi$	$3^3\Pi$
1.9	−0.624 687	−0.531 503	3.9	−0.754 392	−0.745 241
2.0	−0.684 835	−0.588 339	4.0	−0.755 509	−0.744 900
2.1	−0.723 970	−0.624 696	4.1	−0.756 746	−0.744 052
2.2	−0.747 972	−0.669 697	4.2	−0.758 323	−0.742 807
2.3	−0.761 901	−0.700 974	4.3	−0.760 152	−0.741 382
2.4	−0.770 119	−0.720 768	4.5	−0.764 169	−0.738 889
2.5	−0.773 746	−0.730 490	4.7	−0.767 856	−0.737 221
2.6	−0.775 137	−0.733 207	5.0	−0.772 067	−0.735 951
2.7	−0.774 718	−0.731 679	5.1	−0.773 232	−0.735 689
2.8	−0.772 730	−0.728 316	5.2	−0.774 182	−0.735 488
2.9	−0.769 450	−0.725 026	6.0	−0.778 236	−0.734 602
3.0	−0.765 253	−0.723 269	6.1	−0.778 464	−0.734 527
3.1	−0.760 566	−0.724 279	6.2	−0.778 657	−0.734 459
3.2	−0.755 872	−0.731 437	6.4	−0.778 958	−0.734 335
3.3	−0.751 768	−0.737 029	6.6	−0.779 175	−0.734 224
3.4	−0.749 021	−0.740 973	7.2	−0.779 427	−0.733 818
3.5	−0.748 284	−0.743 331	7.4	−0.779 484	−0.733 759
3.6	−0.749 985	−0.744 129	7.6	−0.779 520	−0.733 705
3.7	−0.751 739	−0.744 733	7.8	−0.779 546	−0.733 658
3.8	−0.753 237	−0.745 109	8.0	−0.779 568	−0.733 621

[a]Add −112 to get the total energy.

dx.doi.org/10.1021/jp312359c | J. Phys. Chem. A XXXX, XXX, XXX−XXX

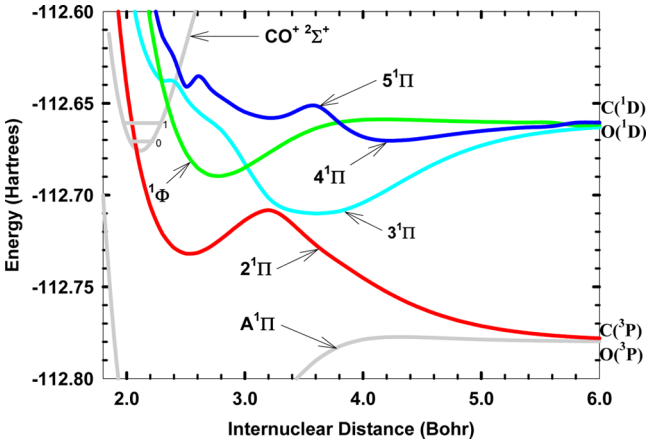

Figure 2. $^1\Pi$ and $^1\Phi$ states of CO with the ion ground state.

eV above the asymptote. Spectroscopic constants for both of these curves are given in Table 2. The minimum of the well in $2^1\Pi$ lies above the asymptote, and these vibrational levels may be short-lived.

The initial capture state for DR from $v = 0$ at low electron energies is clearly $2^1\Pi$, although $3^1\Pi$ may play a role near 0.8 eV.

Calculations in $^1A_1$ symmetry show that the $2^1\Sigma^+$ or D′ state is likely to be an important DR route. However, for this state, the cc-pVQZ basis provides significant Rydberg character to $2^1\Sigma^+$ in the energy region below the ion. For this reason, the most diffuse contracted functions in the s and p sets were removed from the C and O bases. These functions are single primitives, and they were kept in the other contracted functions. The basis set for the $^1A_1$ calculations was therefore 4s, 3p, 3d, 2f, 1g (43321). The CASSCF orbitals were determined by averaging over the lowest six roots in $^1A_1$ symmetry of C_{2v} at all R except for $R > 6.4$, where the orbitals were averaged over the lowest three roots. In the MRCI calculations at the ion R_e, the second and fourth routes are $^1\Delta$ state and the others are $^1\Sigma^+$. The lowest $^1\Sigma^+$ state is the ground state, and the energy at its minimum (−113.147 716) is used to calculate the T_e values for the $^{1,3}A_1$ states in Table 2. The state of interest, $D'^1\Sigma^+$, is the third root. The MRCI potential curves are shown in Figure 3 with the ion ground state. The Davidson-corrected MRCI energies for $D'^1\Sigma^+$ are given in Table 4. The

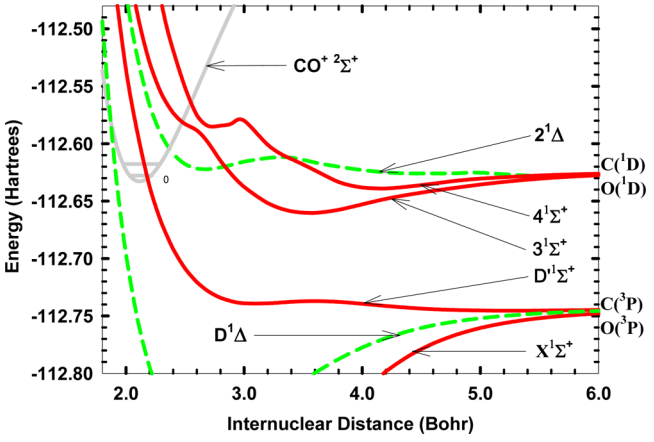

Figure 3. $^1\Sigma^+$ (red, solid lines) and $^1\Delta$ (green, dashed lines) states of CO with the ion ground state.

spectroscopic constants are in Table 2. In order to position the ion correctly in the plots for this basis, the ion curve in Table 1 was shifted upward so as to be at the experimental[13] T_e above the 43321 ground state minimum given above.

From Figure 3, it is clear that the D′ state has a favorable intersection with the ion $v = 0$ level. The D′ state also has a small hump of 1349 cm^{-1} (0.1673 eV) at $3.6037a_0$. The minimum in D′ is 0.1053 eV above the asymptote. $D^1\Delta$ and $2^1\Delta$ are not likely to be important for DR because there is no repulsive Δ state with a favorable intersection that could serve as a feeder state (through a high lying vibrational level of a low n Rydberg state) to the D and 2 states.[14] $3^1\Sigma^+$ is unlikely to play a role in DR at electron energies below 1.8 eV above $v = 0$.

The $^3A_1$ states, $^3\Sigma^+$ and $^3\Delta$, are shown in Figure 4. These states were calculated with the same basis as the $^1A_1$ states. The orbitals were determined in a $^3A_1$ CASSCF which averaged over the lowest eight roots. The eight root MRCI energies with the Davidson correction are shown in Figure 4. Clearly there is no favorable direct recombination route from $v = 0$ at electron energies below 1.6 eV. Indirect recombination may lead to some cross-section structure due to DR along $2^3\Sigma^+$, but it is likely to be in a narrow energy range and is not expected to affect the rate constant.

III. ATOMIC PRODUCTS OF DR

Dissociation along $2^3\Pi$ can lead to ground state atoms if the flux remains on this curve (see Figure 1). However, near $3.5a_0$ an avoided crossing with $3^3\Pi$ can lead to C(^{1}D) and O(^{3}P). Dissociation along $3^3\Pi$ leads directly to C(^{1}D) and O(^{3}P), but three avoided crossings with other states can also lead to C(^{1}D) + O(^{3}P) and C(^{3}P) + O(^{1}D). From $v = 0$ at 0 eV electron energy, the hottest atoms are generated with a combined 2.92 eV of translational energy of which 1.67 eV goes to C(^{3}P) and 1.25 eV goes to O(^{3}P). For the C(^{1}D) + O(^{3}P) asymptote, 1.66 eV is shared between C (0.95 eV) and O (0.71 eV). For the C(^{3}P) + O(^{1}D) asymptote, 0.953 eV is shared between C (0.54 eV) and O (0.41 eV).

Dissociation along $2^1\Pi$ from $v = 0$ will only generate ground state atoms unless the electron energy is above 0.2961 eV, at which the C(^{1}D) + O(^{1}D) asymptote becomes accessible. A traversal of the avoided crossing with $3^1\Pi$ near $R = 3.2a_0$ (see Figure 2) is needed to reach this limit.

For the $^{1,3}A_1$ states in Figure 3, only the D′ state may be an important DR route and it will only generate ground state atoms.

IV. COMPARISON TO PRIOR RESEARCH

A review of early theoretical research can be found in the paper of O'Neil and Schaefer.[17] While early calculations[17] are of a much smaller scale than the current calculations, there is considerable qualitative agreement. They[17] reported full CI minimal basis calculations and found that the second, third, and fourth $^3\Sigma^+$ states are repulsive in agreement with the results reported here. Also, they found a broad peak in the $A^1\Pi$ state of 1140 cm^{-1} near $3.8a_0$ compared to a value of 543 cm^{-1} found here at $4.3081a_0$. (From experimental spectra[18] a minimum value for the hump is 350 cm^{-1} and a maximum value based upon a "crude extrapolation"[18] is 950 ± 150 cm^{-1}.) The $2^3\Pi$ and $3^1\Pi$ states show an avoided crossing near $3.4a_0$, and $2^1\Pi$ crosses the ion near the inner turning point of $v = 0$ as is found in the current study. The $2^3\Pi$ state crosses the ion inner wall above $v = 0$ in agreement with the curve reported here. The

dx.doi.org/10.1021/jp312359c | J. Phys. Chem. A XXXX, XXX, XXX−XXX

Table 4. Energies (au)[a] for $2^1\Pi$ and $D'^1\Sigma^+$

R (bohr)	$2^1\Pi$	$D'^1\Sigma^+$	R (bohr)	$2^1\Pi$	$D'^1\Sigma^+$
1.8	−0.492 006	−0.349 985	4.6	−0.764 332	−0.744 125
1.9	−0.579 726	−0.456 733	4.8	−0.768 305	−0.744 826
2.0	−0.640 929	−0.535 169	5.0	−0.771 321	−0.745 225
2.1	−0.681 229	−0.592 010	5.2	−0.773 579	−0.745 416
2.2	−0.705 992	−0.637 304	5.4	−0.775 254	−0.745 371
2.3	−0.720 783	−0.668 784	5.6	−0.776 485	−0.745 196
2.4	−0.728 726	−0.691 844	5.8	−0.777 384	−0.744 988
2.5	−0.731 888	−0.708 583	6.0	−0.778 037	−0.744 749
2.6	−0.731 447	−0.720 520	6.2	−0.778 507	−0.744 503
2.7	−0.728 451	−0.728 767	6.4	−0.778 806	−0.744 275
2.8	−0.723 873	−0.734 166	6.6	−0.779 055	−0.743 945
2.9	−0.718 654	−0.737 380	6.8	−0.779 249	−0.743 768
3.0	−0.713 753	−0.738 959	6.9	−0.779 266	
3.2	−0.708 200	−0.738 967	7.0	−0.779 310	−0.743 617
3.4	−0.715 623	−0.737 675	7.2	−0.779 460	−0.743 492
3.6	−0.727 155	−0.737 031	7.4	−0.779 523	−0.743 388
3.8	−0.736 587	−0.737 730	7.6	−0.779 568	−0.743 303
4.0	−0.745 140	−0.739 386	7.8	−0.779 599	−0.743 234
4.2	−0.752 784	−0.741 264	8.0	−0.779 621	−0.743 178
4.4	−0.759 202	−0.742 887			

[a]Add −112 to get the total energy.

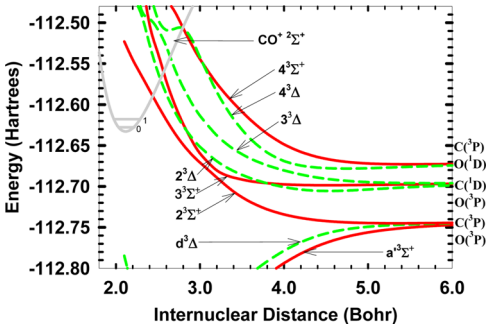

Figure 4. $^3\Sigma^+$ (red, solid lines) and $^3\Delta$ (green, dashed lines) states of CO with the ion ground state.

$3^3\Pi$ state crosses near the inner turning point of $v = 0$, but the curve reported here crosses near the outer turning point. The $4^3\Pi$ state appears to be close to the $3^3\Pi$ near the ion, which the current calculations do not find. They show that the $D'^1\Sigma^+$ state has a favorable crossing with the $v = 0$ level of the ion, which is also found here. They found $2^3\Sigma^+$ and $2^3\Delta$ crossing the outer wall of the ion above $v = 0$ as found here. Lastly, their D and $2^1\Delta$ states cross the ion above $v = 0$ as found here.

Another early paper[19] using Hartree−Fock orbitals and a limited CI did not report the repulsive states of interest here but did report spectroscopic constants for several states. For the states listed here in Table 2, their T_e values compare quite favorably, with the exception of the A state which is 0.67 eV too high. For the a′ and d states the T_e values of 6.89 and 7.51 eV are better than those reported here (see Table 2) and may be due to the presence of Rydberg character (which is intentionally omitted here) in the basis set.[20] Their R_e values are further from experiment than those reported here, except for the a′ and d states. Some of their ω_e values are considerably further from experiment than those reported here. For example, the neutral ground state differs by 169 cm^{-1} and the A state by 289 cm^{-1} from experiment but the a′ and d state values are close to those calculated here. The accuracy of these early calculations for the a′ and d states is remarkable.

The D′ and C′ (here labeled $3^1\Sigma^+$) states have been the subject of prior calculations[21] using a large Slater basis set with diffuse functions. Orbitals were obtained in MCSCF calculations on $A^1\Pi$, and the CI was generated by taking excitations into a partitioned orbital space. They reported an outer hump in D′ of 0.205 eV at $3.75a_0$. The hump calculated here is 0.038 eV smaller and is at $0.15a_0$ smaller R. A secondary minimum at $3.145a_0$ and 0.092 eV above its asymptote was reported compared to the values found here of $3.0895a_0$ and 0.105 eV above the asymptote. They found a primary minimum at smaller R due to Rydberg character, which is not present in these calculations. The T_e of 11.11 eV is the same value obtained here (see Table 2). The estimated value for ω_e of 550 cm^{-1} compares well to the value found here of 523.9 cm^{-1}. For C′ (labeled $3^1\Sigma^+$ here) they reported an outer well with T_e, R_e, and ω_e of 13.34 eV, $3.619a_0$, and an estimated 600 cm^{-1}, in good agreement with the values found here of 13.26, $3.5577a_0$, and 654 cm^{-1}, respectively. They commented that this well may be too high. An inner well due to Rydberg character was found. The $A^1\Pi$ state has T_e, R_e, ω_e, and $\omega_e x_e$ of 8.28 eV, $2.362a_0$, 1475 cm^{-1}, and 18.9 cm^{-1} and does not compare as well with experiment as the values reported here (see Table 2), with the exception of $\omega_e x_e$. $A^1\Pi$ also has a maximum of 838 cm^{-1} at $4.31a_0$ compared to the value found here of 543 cm^{-1} at $4.3081a_0$. The peak found in $E^1\Pi$ (labeled here $2^1\Pi$) of 2.18 eV at $3.20a_0$ is in agreement with the results found here (see above). The $2^1\Pi$ minimum found here at $2.5347a_0$ does not appear in their curve due to mixing with Rydberg character.

The only storage ring experiment[23] on CO^+ DR was reported in 1998 when there was much less theoretical guidance available than there is today. The experiment was done on $^{13}CO^+$. The results reported here show that the DR of CO^+ will occur on potential curves of $^{1,3}\Pi$ and $^1\Sigma^+$ symmetry. Since the ground state has $^2\Sigma^+$ symmetry, the free electron must have $p\pi$ or $d\pi$ symmetry to form $^{1,3}\Pi$ states and $s\sigma$, $p\sigma$, or $d\sigma$ symmetry to form the $^1\Sigma^+$ state. Higher values of the angular momentum

dx.doi.org/10.1021/jp312359c | J. Phys. Chem. A XXXX, XXX, XXX−XXX

will be less important because of small electron capture widths. In the derivation of the product quantum yields from the storage ring data, product distributions were fit using model isotropic, $\sin^2\theta$, and $\cos^2\theta$ angular distributions, where θ is the angle between the internuclear axis and the space fixed axis in the direction of the electron beam. This corresponds to using only sσ, pπ, and pσ electron waves, respectively.[22] However, capture by dπ and dσ electron partial waves (corresponding to $\sin^2\theta\cos\theta^2$ and $(3\cos^2\theta - 1)^2$ atomic product distributions, respectively) is quite likely[22] but was ignored in the derivation of quantum yields. At zero electron energy, this omission is not important because the product angular distributions are expected to be mostly isotropic. Indeed, Figure 4 of ref 23 shows good agreement between the measured product distributions and the model distributions. At nonzero electron energies where the direction of the electron beam is well-defined relative to the ion, the product distribution is anisotropic. For nonzero electron energies, Figure 5 of ref 23 shows considerably less agreement between the measured and fitted model distributions and the decreased agreement may be due to the omission of dπ and dσ electron partial waves in the model. The decreased agreement has been attributed to "sharply reduced count rates"[23] at nonzero energies.

Since theoretical quantum yields will be reported separately, a quantitative comparison with the storage ring[23] results is not yet possible. However, the storage ring finding that, at 0 eV electron energy, 76% of the DR events lead to ground state atoms and no O(^{1}S) is observed is in qualitative agreement with the results reported here. Of the four important dissociative routes identified in this paper, only ground state atoms are generated from D$'^1\Sigma^+$ and from $2^1\Pi$ below 0.2961 eV electron energy. Along $2^3\Pi$, mostly ground state atoms will result as long as the dissociating flux remains on the adiabatic curve, as it is likely to do.

Rosen et al.[23] pointed out a large disagreement between a model potential[24] for the diabatic D′ state derived from experimental data and an ab initio calculation using Hartree–Fock orbitals and a single CI.[25] In the model, the D′ state crosses the ion at the large R turning point of the $v = 0$ level, but in the latter calculation, it crosses at the inner turning point of $v = 2$. The results reported here (see Figure 3) show that the crossing occurs near the large R turning point of $v = 0$, in agreement with the model potential (but slightly to smaller R) and in clear disagreement with the ab initio result. The ab initio calculation[25] also does not display a hump for $R < 4$ Å and is purely repulsive in disagreement with the results reported here. From experimental data, the model found the outer hump in the D′ state to be between 0.106 and 0.1588 eV above the asymptote compared to the value found here of 0.167 eV. The ab initio calculation[25] showed the $2^1\Pi$ curve crossing the ion at the outer turning point of $v = 0$ in agreement with the result reported here (but slightly to smaller R).

Calculations on the D and $2^1\Delta$ states have been reported[26] using the approach described above.[21] The spectroscopic constants for the D state are in good agreement with those calculated here except for ω_e, which is 56 cm^{-1} below the experimental value compared to 14 cm^{-1} below for the value reported here (see Table 2). For $2^1\Delta$, the T_e is 0.59 eV below that calculated here and the other spectroscopic constants are not similar to those reported here, probably reflecting the importance of Rydberg character in their adiabatic calculation. This character is intentionally omitted here in order to obtain a diabatic valence state. The importance of Rydberg character is evident in their calculated ω_e of 2198 cm^{-1} which is very similar to that for the ion.

A correlation scaled plus extrapolation[27] approach has been applied to the $A^1\Pi$ state and yields a barrier height of 594 ± 46 cm^{-1} at 4.25 ± 0.05a_0 in good agreement with the result obtained here. The calculated R_e is 2.3331 ± 0.0028a_0 and is an improvement over the value found here of 2.3426a_0.

A recent calculation[28] used an aug-cc-pVQZ[9] basis supplemented with diffuse functions. The orbitals were determined in single configuration SCF calculations. The CI wave function was generated by taking all single and double excitations from a multiconfiguration reference space composed of configurations chosen with an energy selection criterion. The Davidson correction was used. The energy of the neutral ground state is −113.176 156 58 at the experimental R_e and is above the value calculated here of −113.189 044 at the calculated R_e, which is only 0.0072a_0 from the experimental R_e. Rydberg character, intentionally omitted here, plays a greater role in the energy of high lying valence states compared to low lying states. The reported calculations have improved spectroscopic constants (with the exception of T_e) compared to those calculated here for the D′ state. Spectroscopic constants for C$'^1\Sigma^+$ (here labeled $3^1\Sigma^+$), although uncertain, compare favorably to those calculated here. The E$'^1\Pi$ state (labeled $2^1\Pi$ here) has a jagged structure compared to the smooth valence curve calculated here. This is in part due to Rydberg character. The $3^1\Pi$ valence state has a broad well similar to that calculated here. No spectroscopic constants were reported for $3^1\Pi$. Potential curves for the k$^3\Pi$ (labeled $2^3\Pi$ here) and $3^3\Pi$ states have an avoided crossing near 3.5a_0 with a double minimum in the upper state, not found here. The minimum in the k state is at 11.220 eV with an R_e of 2.519a_0, in good agreement with the values found here of 11.26 eV and 2.6248a_0. Their smaller R_e is probably due to diffuse functions. $4^3\Pi$ (labeled here $3^3\Pi$) falls at 12.35 eV, only 0.05 eV from the minimum in the state calculated here. The R_e value of 2.65 compares well to our value of 2.6041a_0.

Using an approach similar to that described here, comparable spectroscopic constants were found for the X, A, a′, and d states.[29] No other states were reported. The barrier in the A state was found to be 792 cm^{-1} at 4.2a_0.

A diabatic Morse potential[30] for the E$'^1\Pi$ state (labeled $2^1\Pi$ here) derived from spectroscopic data found a minimum at 2.31a_0 compared to a value of 2.5347a_0 found here. The difference may be due to Rydberg character which is intentionally omitted here. For $^{12}C^{16}O$, I found a force constant and an anharmonicity of 1116 and 16.99 cm^{-1}, respectively. The calculated T_e is 100 290 cm^{-1} compared to 98 176.0 cm^{-1} found for the diabatic Morse potential.

Dissociation along $2^3\Pi$ appears to account for the results of a photodissociation experiment[31] that found evidence for a repulsive $^3\Pi$ state at about 1.8 eV below the bottom of the ion potential well leading to C(^{1}D). The relevant curve appears to be $2^3\Pi$ (see Figure 1).

V. CONCLUSIONS

Based solely upon proximity to the ion, four states dominate the DR of $v = 0$: $2^3\Pi$, $3^3\Pi$, $2^1\Pi$, and D$'^1\Sigma^+$. A final assessment of the importance of these states for DR awaits the calculation of electron capture widths and cross sections, which will be published separately.

Although quantum yields will be presented in a future paper, the storage ring[23] result that most of the recombinations

dx.doi.org/10.1021/jp312359c | J. Phys. Chem. A XXXX, XXX, XXX–XXX

produce ground state atoms is in agreement with the results reported here.

A $^3\Pi$ state arises from the C(^{1}S) + O(^{3}P) limit. This state is not calculated here but has an asymptote that is 0.24 eV (0.0088 au) below the ion $v = 0$ level. From the potential curves in Figure 1 is appears unlikely that this limit can be reached starting from $2^3\Pi$ or $3^3\Pi$ and after traversing several curve crossings. It is therefore unlikely that C(^{1}S) can be generated from DR of $v = 0$ at electron energies between 0 and 1 eV. Surprisingly, the storage ring experiment[23] found a yield of 5% (with an error of 30%) for C(^{1}S) at 1.0 eV. Also, the energetics prohibit the generation of O(^{1}S) from $v = 0$ for these energies in agreement with the storage ring result.

The generation of excited atoms (O(^{1}D) and C(^{1}D)) at electron energies below 0.2961 eV requires DR via the $2^3\Pi$ and $3^3\Pi$ states and is responsible for C(^{1}D), detected by the International Ultraviolet Explorer and attributed[3] to DR of CO^+.

AUTHOR INFORMATION

Corresponding Author

*Phone: (781) 368-9080. E-mail: slg@sci.org.

Notes

The authors declare no competing financial interest.

ACKNOWLEDGMENTS

This research is supported by the National Science Foundation under Grant ATM-0838061 and by NASA under Grant NNX09AQ73G.

REFERENCES

(1) Latter, W. B.; Walker, C. K.; Maloney, P. R. Detection of the Carbon Monoxide Ion (CO^+) in the Interstellar Medium and a Planetary Nebulae. *Astrophys. J.* **1993**, *419*, L97−L100.

(2) Giguere, P. T.; Huebner, W. F. A Model of Comet Comae. I—Gas-Phase Chemistry in One Dimension. *Astrophys. J.* **1978**, *223*, 638−654. Huebner, W. F.; Giguere, P. T. A Model of Comet Comae. II—Effects of Solar Photodissociative Ionization. *Astrophys. J.* **1980**, *238*, 753−762.

(3) Woods, T. N.; Feldman, P. D.; Dymond, K. F. The Atomic Carbon Distribution in the Coma of Comet P/Halley. *Astron. Astrophys.* **1987**, *187*, 380−384.

(4) Eviatar, A.; Goldstein, R.; Young, D. T.; Balsiger, H.; Rosenbauer, H.; Fuselier, S. A. Energetic Ion Fluxes in the Inner Coma of Comet P/Halley. *Astrophys. J.* **1989**, *339*, 545−557.

(5) Keller, C. N.; Cravens, T. E. Plasma Density Enhancement at the Comet Halley Diamagnetic Cavity Boundary. *J. Geophys. Res.* **1990**, *95*, 18755−18768.

(6) Paxton, L. J. *Atomic Carbon in the Venus Thermosphere: Observations and Theory*. Ph.D. Thesis, University of Colorado, Denver, 1983.

(7) Fox, J. L.; Hac, A. Velocity Distributions of C Atoms in CO^+ Dissociative Recombination: Implications for Photochemical Escape of C from Mars. *J. Geophys. Res.* **1999**, *104*, 24729−24738.

(8) Krasnopolsky, V. A.; Cruikshank, D. P. Photochemistry of Triton's Atmosphere and Ionosphere. *J. Geophys. Res.: Planets* **1995**, *100*, 21271−21286.

(9) Dunning, T. H., Jr. Gaussian basis sets for use in correlated molecular calculations. I. The atoms boron through neon and hydrogen. *J. Chem. Phys.* **1989**, *90*, 1007−1023.

(10) MOLPRO is a package of ab initio programs written by H.-J. Werner and P. J. Knowles, with contributions from R. D. Amos, A. Bernhardsson, A. Berning, et al. MOLPRO-2000.1.

(11) Werner, H.-J.; Knowles, P. J. A Second Order Multi-configuration SCF Procedure with Optimum Convergence. *J. Chem. Phys.* **1985**, *82*, 5053−5063. Knowles, P. J.; Werner, H.-J. An Efficient Second-Order MC SCF Method for Long Configuration Expansions. *Chem. Phys. Lett.* **1985**, *115*, 259−267.

(12) Werner, H.-J.; Knowles, P. J. An efficient internally contracted multiconfiguration-reference configuration interaction method. *J. Chem. Phys.* **1988**, *89*, 5803. Knowles, P. J.; Werner, H.-J. An efficient Method for the Evaluation of Coupling Coefficients in Configuration Interaction Calculations. *Chem. Phys. Lett.* **1988**, *145*, 514−522.

(13) Huber, K. P.; Herzberg, G. *Molecular Spectra and Molecular Structure, IV. Constants of Diatomic Molecules*; Van Nostrand Reinhold: New York, 1979.

(14) Guberman, S. L. Spectroscopy Above the Ionization Threshold: Dissociative Recombination of the Ground Vibrational Level of N_2^+. *J. Chem. Phys.* **2012**, *137* (074309), 1−16.

(15) Moore, C. E. *Natl. Bur. Stand. Circ. (U. S.)* **1949**, No. 467.

(16) Berden, G.; Jongma, R. T.; van der Zande, D.; Meijer, G. A reanalysis of the $k^3\Pi$ state of CO. *J. Chem. Phys.* **1997**, *107*, 8303−8310.

(17) O'Neil, S. V.; Schaefer, H. F., III. Valence-Excited States of Carbon Monoxide. *J. Chem. Phys.* **1970**, *53*, 3994−4004.

(18) Simmons, J. D.; Bass, A. M.; Tilford, S. G. The Fourth Positive System of Carbon Monoxide Observed in Absorption at High Resolution in the Vacuum Ultraviolet Region. *Astrophys. J.* **1969**, *155*, 345−358.

(19) Hall, J. A.; Schamps, J.; Robbe, J. M.; Lefebvre-Brion, H. Theoretical Study of the Perturbation Parameters in the $a^3\Pi$ and $A^1\Pi$ States of CO. *J. Chem. Phys.* **1973**, *59*, 3271−3283.

(20) Huo, W. M. Electronic Structure of the First Excited State of CO. I. SCF Wavefunction Calculated in the Restricted Hartree-Fock Formalism. *J. Chem. Phys.* **1966**, *45*, 1554−1564.

(21) Cooper, D. L.; Kirby, K. Theoretical Study of Low-Lying $^1\Sigma^+$ and $^1\Pi$ States of CO. I. Potential Energy Curves and Dipole Moments. *J. Chem. Phys.* **1987**, *87*, 424−432.

(22) Guberman, S. L. Product Angular Distributions in Dissociative Recombination. *J. Chem. Phys.* **2004**, *120*, 9509−9513.

(23) Rosén, S.; Peverall, R.; Larsson, M.; Le Padellec, A.; Semaniak, J.; Larson, Å.; Strömholm, C.; van der Zande, W. J.; Danared, H.; Dunn, G. H. Absolute Cross Sections and Final-State Distributions for Dissociative Recombination and Excitation of CO^+ ($v = 0$) Using an Ion Storage Ring. *Phys. Rev. A: At. Mol. Opt. Phys.* **1998**, *57*, 4462−4471.

(24) Tchang-Brillet, W.-Ü. L.; Julienne, P. S.; Robbe, J. M.; Letzelter, C.; Rostas, F. A Model of the $B^1\Sigma^+$−$D'^1\Sigma^+$ Rydberg−Valence Predissociating Interaction in the CO Molecule. *J. Chem. Phys.* **1992**, *96*, 6735−6745.

(25) Hiyama, M.; Nakamura, H. Superexcited States of CO Near the First Ionization Threshold. *Chem. Phys. Lett.* **1996**, *248*, 316−320. Hiyama, M.; Kosugi, N.; Nakamura, H. Characteristics and Dynamics of Superexcited States of Diatomic Molecules: General Theoretical Procedure. *J. Chem. Phys.* **1997**, *107*, 9370−9381.

(26) Rosenkrantz, M. E.; Kirby, K. Theoretical Study of Low-Lying $^1\Sigma^-$ and $^1\Delta$ States of CO. *J. Chem. Phys.* **1989**, *90*, 6528−6532.

(27) Varandas, A. J. Accurate Ab Initio Potentials at Low Cost via Correlation Scaling and Extrapolation: Application to CO($A^1\Pi$). *J. Chem. Phys.* **2007**, *127*, 114316.

(28) Vázquez, G. J.; Amero, J. M.; Liebermann, H. P.; Lefebvre-Brion, H. Potential Energy Curves for the $^1\Sigma^+$ and $^{1,3}\Pi$ States of CO. *J. Phys. Chem. A* **2009**, *113*, 13395−13401.

(29) Majumder, M.; Sathyamurthy, N.; Lefebvre-Brion, H.; Vázquez, G. J. Photoabsorption of Carbon Monoxide: A Time-Dependent Quantum Mechanical Study. *J. Phys. B: At. Mol. Opt. Phys.* **2012**, *45*, 185101.

(30) Lefebvre-Brion, H.; Eidelsberg, M. New Experimental Study and Theoretical Model of The Extreme UV Absorption Spectrum of CO Isotopologs. *J. Mol. Spectrosc.* **2012**, *271*, 59−65.

(31) Forch, B. E.; Merrow, C. N. Photodissociation Processes in Carbon Monoxide at 193 nm. *J. Chem. Phys.* **1991**, *95*, 3252−3257.

566 (32) Wolk, G. L.; Rich, J. W. Observation of a New Electronic State
567 of Carbon Monoxide Using LIF on Highly Vibrationally Excited
568 CO(X $^1\Sigma^+$). *J. Chem. Phys.* **1983**, *79*, 12−18.